Available online at www.sciencedirect.com

ScienceDirect

Advances in Space Research xxx (xxxx) xxx

ADVANCES IN SPACE RESEARCH (a COSPAR publication)

www.elsevier.com/locate/asr

Correlation between f_oE_s and zonal winds over Rome, Okinawa and Townsville using Horizontal Wind Model (HWM14) during solar cycle 22

Bushra Gul [a,*], Muhammad Ayyaz Ameen [a,b], Tobias G.W. Verhulst [c]

[a] University of Karachi, Karachi, Pakistan
[b] Pakistan Space and Upper Atmosphere Research Commission (SUPARCO), P.O. Box 8402, Karachi, Pakistan
[c] Royal Meteorological Institute (RMI), 3 Avenue Circulaire, b-1180 Brussels, Belgium

Received 25 June 2021; received in revised form 7 August 2021; accepted 19 August 2021

Abstract

The relation between ionosonde critical frequency of ionospheric sporadic E-layer (f_oE_s) and disturbed zonal wind is studied over Okinawa (26.68°N, 128.15°E), Rome (41.98°N, 12.49°E) and Townsville (19.63°S, 146.8°E) during different solar activity years, 1987 (moderate), 1996 (low) & 2001 (high) (Okinawa and Townsville) and 1987 (moderate), 1995 (low) & 2000 (high) (Rome). The variation of monthly hourly medians of f_oE_s shows annual trend with maximum values in local summer. However, it does not show dependence on solar activity. The correlation is studied between median f_oE_s values and the zonal winds obtained from climatological Horizontal Wind Model (HWM14). The strong correlation coefficients obtained between the parameters suggest that HWM14 may be used as a proxy to predict the climatology of the sporadic layers. A more comprehensive study based upon the same procedure is planned in future.

Keywords: Sporadic E-layer; Horizontal Wind Model; Disturbed zonal wind

1. Introduction

The occurrence of sporadic-E (E_s) layer is important for space weather research due to its high electrical conductivity and significant impact on modern radio communications (Dalakishvili et al., 2020). Several theoretical and experimental studies have been carried out, describing different phenomena associated with formation and occurrence of E_s-layer with limited thickness (a few km). On ionograms, the E_s-layer appears as a strong reflection that can occur over a range of heights from about 90 to 120 km or more. The maximum frequency reflected from E_s-layer can be greater than the critical frequency of any of the normal layers (Piggott and Rawer, 1972). E_s-layers are not rare as the name perhaps implies, but rather a regularly occurring phenomenon over a large range of latitudes. They can appear at almost any time but exhibit distinctive seasonal patterns (Schunk and Nagy, 2009). Wind shear is considered to be the main physical mechanism for E_s-layer formation (Dalakishvili et al., 2020, and the references therein). According to this theory, in the lower thermosphere the eastward wind at lower heights changes to the westward at upper heights, or the southward wind changes to the northward, which causes the accumulation of the heavy metallic ions into the horizontal thin layer in the regions close to the wind polarization changes (Haldoupis, 2012). The primary source of E_s ionization are meteoric metal atoms that are deposited over a broad range of heights around 100 km (Whitehead, 1989; Plane et al., 2003).

* Corresponding author.
E-mail address: bushraagul3@gmail.com (B. Gul).

https://doi.org/10.1016/j.asr.2021.08.027
0273-1177/

Please cite this article as: B. Gul, M. A. Ameen and T. G. W. Verhulst, Correlation between f_oE_s and zonal winds over Rome, Okinawa and Townsville using Horizontal Wind Model (HWM14) during solar cycle 22, Advances in Space Research, https://doi.org/10.1016/j.asr.2021.08.027

The fraction of these atoms that become ionized are relatively long-lived (several hours), allowing them to be concentrated by wind shears, or other forces, into thin, dense layers. Thunderstorms are suspected to have some influence on local E_s-layers which are created as a result of lightning (Davis and Johnson, 2005). Atmospheric gravity waves may even act to enhance wind shear (Didebulidze et al., 2020). Similarly, meteor showers might directly influence the E_s-layer, since they affect the available supply of long-lived metallic ions. Such factors result in occurrence of E_s with respect to latitude, longitude, altitude and local time (Haldoupis, 2011). However, this paper will only be concerned with the climatology of E_s-layers, without discussing their behaviour on shorter time scales.

The Horizontal Wind Model (HWM) is an empirical model of horizontal winds, based on wind-imaging interferometer (WINDII) green line observations between 90 and 120 km (Drob et al., 2015). The model includes mean winds, solar diurnal and semi-diurnal tides, and some planetary wave components, as well as annual and semiannual variations in these fields. As an empirical spectral climatology, the HWM represents the predominant repeatable oscillations of the atmosphere (day-to-day and year-to-year). It makes use of geophysical indices such as solar radio flux (F10.7 cm), or the magnetic index (Ap). HWM provides a framework for the statistical inter-comparison and validation of various upper atmospheric measurements and theoretical models. HWM also provides background wind fields for studies of wave propagation, first principles ionospheric models, ionospheric data assimilation systems, and studies of large and small scale ionospheric processes such as dynamo electric fields, Drob et al. (2008). The HWM has been updated using new ground-based data from the equatorial and polar regions, as well as cross track winds from the satellite (Drob et al., 2015). The ground-based measurements fill latitudinal data gaps in the prior observational database. The updated version of model, HWM14 provides an improved time-dependent, observational based, global empirical specification of the upper atmospheric general circulation patterns and migrating tides. In basic agreement with existing accepted theoretical knowledge of the thermosphere general circulation, additional calculations indicate that the empirical wind specifications are consistent with climatological ionosphere plasma distribution and electric field patterns, Drob et al. (2008). Recently, Dalakishvili et al. (2020) showed that HWM may be used to predict the formation of single/double peak in E_s-layer at mid-latitude during nighttime.

The goal of this study is to investigate the relation between the zonal winds obtained from the HWM14 model and the appearance and maximal density of sporadic E-layers. This work is intended as a proof of principle demonstrating how a zonal wind model like HMW14 could be used to predict the climatological behaviour of the sporadic layers. For the purpose, we analyze this relation using data from three selected ionosondes, chosen from different parts of the globe. For each of these ionosondes a long series of high-quality observations is available, covering various levels of solar activity. Being a global climatological model, HWM14 can be used for any location and any period.

2. Data and methodology

For the purpose of this study, we analyse the correlation of the zonal winds with the f_oE_s values from three different ionosondes, located at various latitudes in both the northern and southern hemispheres: Okinawa, Townsville, and Rome (see Table 1). Three different types of ionosondes used to acquire data at these location each made by the respective hosting country. They are the Panoramic Ionospheric Recorder PIR-9B/10A, Advanced Ionospheric Sounder AIS-INGV (National Institute of Geophysics and Volcanology, INGV of Italy) and IPS 4D/5A (Ionospheric Prediction Services, Australia), respectively. Long series of observations are available for each of these observatories, allowing us to investigate the effect of differences in solar activity level. Periods of high, medium, and low solar activity were selected for this work (see Table 2). The years have been chosen on the basis of their solar activity and the availability of f_oE_s data for each station. The ionosonde acquired f_oE_s data sets have been collected from World Data Centre (WDC) hosted by National Institute of Information and Communication Technology (NICT), Japan and Space Weather Services (SWS, formerly IPS), Australia.

The disturbed zonal wind (*dzw*) parameter is the wind velocity in eastward direction obtained for disturbed magnetic conditions. It depends on magnetic latitude, magnetic local time, and Ap (Kp). To estimate the *dzw* values for the selected locations the model was run at a fixed height of 100 km (assuming f_oE_s at the same altitude) and Ap = 30 (for disturbance). Details of codes and background of the model can be found in the report by Drob et al. (2015).

To take into account seasonal effects, the analyses were performed separately for four seasons: June solstice (May-August), December solstice (November-February), March equinox (March-April) and September equinox (September-October). The raw data files of each ionospheric station contained daily hourly values of f_oE_s in universal time. The monthly hourly median of these observations, say for a given month, year and station was obtained by taking the median of all 0000UT values. Likewise, medians of all 24 h were calculated. Such 24 median values gave the monthly hourly median of the given month of the year and station under consideration. The observation time was converted from UT to LT as per offset between the two. The monthly hourly medians of f_oE_s were then used to find seasonal and annual medians as per the chosen months for each season. In case of absence of E_s-layer, NaN (Not a Number) was inserted to avoid illogical medians. Accordingly, the *dzw* daily hourly values were obtained from HWM14 and then synchronized with f_oE_s data sets by calculating medians. Correlation coefficients

Table 1
Locations and instruments used to acquire data.

Station	Geographical coordinates	Geomagnetic Coordinates	Ionosonde
Okinawa	26.6°N, 128.1°E	17.0°N, 198.6°E	9B/10A
Rome	41.9°N, 12.4°E	42.4°N, 94.5°E	AIS-INGV
Townsville	19.6°S, 146.8°E	28.9°S, 220.7°E	4D/5A

r between the parameters have been calculated using Eq. (1):

$$r = \frac{\sum(x_i - \bar{x})(y_i - \bar{y})}{\sqrt{\sum(x_i - \bar{x})\sum(y_i - \bar{y})}} \quad (1)$$

where dzw (m/s) has been considered x and f_oE_s (MHz) is taken as y with corresponding means, accordingly to calculate r.

Additionally, linear regression between the two variables have been represented using slope a and intercept b form of the straight line equation:

$$f_oE_s = a \times dzw + b \quad (2)$$

3. Results

3.1. Variations in f_oE_s

Fig. 1 shows monthly hourly medians of f_oE_s values measured at the included station during different solar epochs. The panels in the first column show ionosonde f_oE_s values over Okinawa, while the middle and last columns represent the critical frequencies over Rome and Townsville, respectively. The years of solar activity have been mentioned on the left hand side of the figure. It is clear from the figure that f_oE_s follows an annual trend, it means that the critical frequency has the peak during local summer in the afternoon hours at all stations and years under study. In general, Okinawa values of f_oE_s are enhanced around noon. The largest station values of f_oE_s are occurring in morning during pre-noon hours over Rome in all years under study. For Townsville there are some events of high f_oE_s values during post-sunset and midnight hours during HSA/MSA and LSA, respectively.

3.2. Correlations between f_oE_s and disturbed zonal wind

Correlation coefficients between f_oE_s and dzw obtained from HWM14 with 100 km fixed altitude over the stations and years under study have been calculated. The seasonal correlation coefficients are given in Table 3. These seasonal correlation coefficients were calculated by comparing hourly medians of both parameters over each season. The annual correlation coefficients along with scatter plots are shown in Fig. 2. Each pane of Fig. 2 is plotted between the annual f_oE_s (dependent variable) and dzw (independent variable) hourly medians calculated over entire year. This means that a point on the plot represents the correlation coefficient between the two parameters at a given hour, hence there are 24 points in each subplot. This corresponds to the relation between annual median of the two parameters per hour with the assumption that dzw is deriving factor of f_oE_s. Table 4 gives the coefficients of the trend line between them as shown in Fig. 2. These coefficients are the slopes and intercepts of the trend line fitted over the points as mentioned in Eq. 2.

Table 2
Solar epochs covered under the study.

Selected Years	Rz	Solar Activity
1996/95	33.9	Low (LSA)
1987	25.1/11.6	Moderate (MSA)
2001/00	173.9/170.4	High (HSA)

It is clear from Table 3 that the correlation coefficients are generally higher at mid-latitude stations in the northern hemisphere (Okinawa and Rome i.e., from 0.59 to 0.89) than over low-latitude station in the southern hemisphere (Townsville, i.e., from 0.10 to 0.76). For Rome, the correlation between magnitudes of f_oE_s and dzw is the highest during March equinox. For example, during LSA the correlation coefficient reaches a value of 0.84. The correlation coefficients decrease in magnitude from March to September equinox. For LSA, it decreases from 0.84 to 0.79. Summer correlation coefficients (0.75 and 0.76, respectively) are higher than winter (0.76 and 0.70, respectively) for MSA and HSA with the least values in September equinox. During LSA, September equinox values are higher than summer and winter.

For Okinawa, the highest correlation coefficients are also seen in March equinox (0.89) for all years under study except during MSA (0.81) where September equinox correlation coefficient is the highest (0.88). Summer correlation coefficients are higher than winter during MSA (0.80) and LSA (0.82).

While looking at correlation coefficients over the southern hemispheric station Townsville, we find that local summer correlation coefficients are the highest during MSA (0.57) and HSA (0.76). In general, for Townsville equinoctial correlation coefficients are lower than the solstice correlation coefficients. This is opposite to the behaviour of correlation coefficients over the northern hemispheric stations under study.

In the northern hemisphere, f_oE_s over Okinawa shows stronger seasonal correlation with dzw than Rome in all seasons and years under study. The magnitude of correlation coefficient over Townsville are least among all stations.

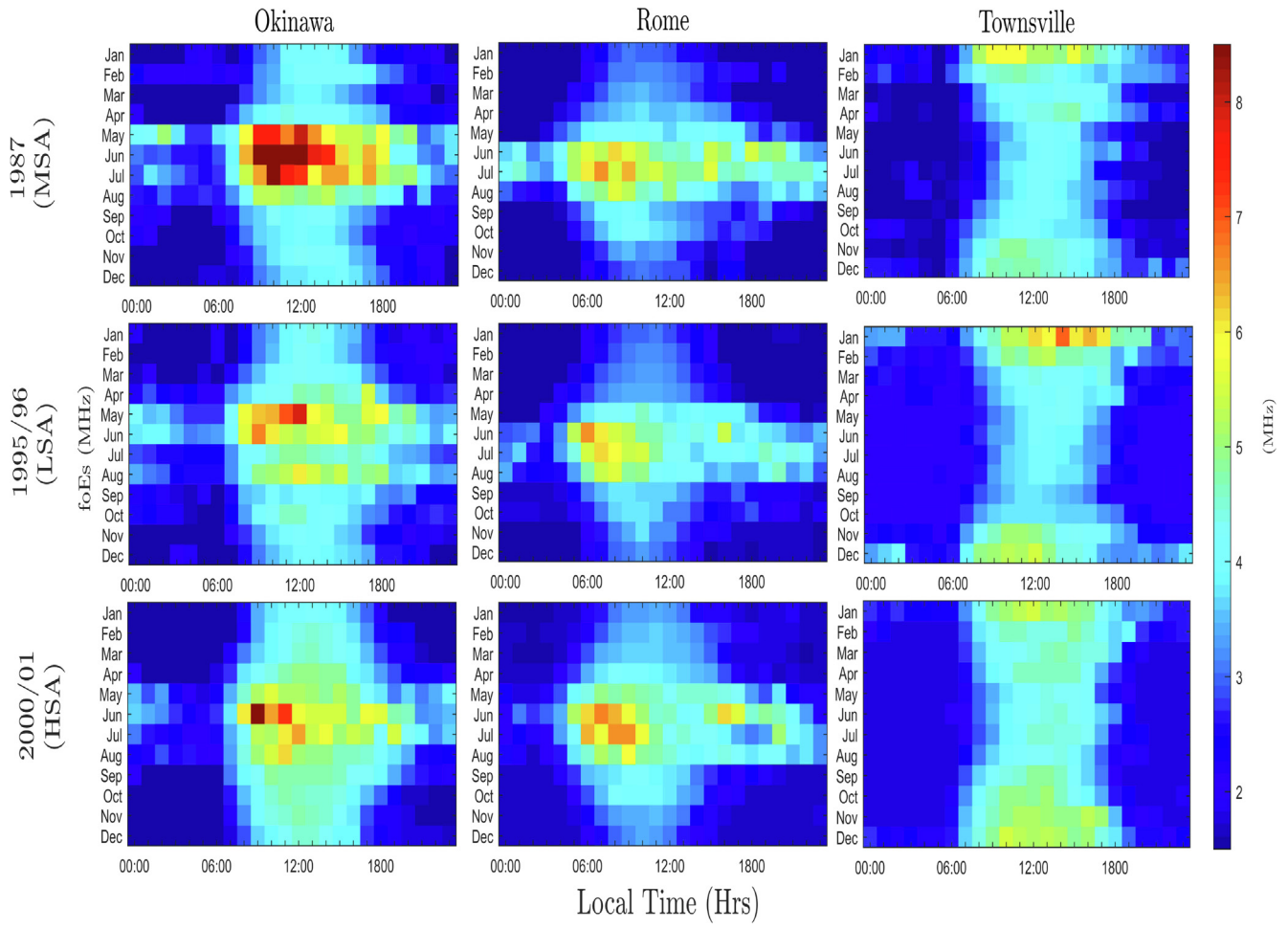

Fig. 1. f_oE_s variation over stations under study. Each pane of the figure shows monthly hourly values (see Section 2) of ionosonde f_oE_s at respective station/year using pseudo. colours scheme.

It can be deduced from Table 3 that *dzw* estimated from HWM14 is highly correlated with the critical frequency of sporadic E over Okinawa, moderately over Rome and the least over Townsville.

Fig. 2 shows that the correlation coefficient is proportional to the solar activity. This means that greater the solar activity, the higher will be the correlation between f_oE_s and *dzw* over a given station under study, in general.

The regression coefficients obtained in Table 4 shows that slope a is greatest during HSA at each station corresponding to greater value of b. Whereas lowest values are observed during LSA. It is observed that both, correlation and regression coefficients are following the latitude. Using HWM14 model as proxy to predict the climatology of sporadic layers is more favourable in the northern hemisphere among the stations under study. We also investigated the correlation as a function of time of day. For this purpose, the data from each station was combined for all years for the time intervals 0080–1600 LT (daytime) and 2000–0400 LT (nighttime). The usual trend was observed (prominent during the day than that of nighttime).

Table 3
Correlation coefficients between seasonal f_oE_s and *dzw* at 100 km.

	Jun Sol	Dec Sol	Mar Eqn	Sep Eqn
		Rome		
1987 (MSA)	0.75	0.74	0.77	0.61
1995 (LSA)	0.59	0.63	0.84	0.79
2000 (HSA)	0.76	0.70	0.78	0.64
		Okinawa		
1987 (MSA)	0.80	0.78	0.81	0.88
1996 (LSA)	0.82	0.80	0.89	0.72
2001 (HSA)	0.75	0.84	0.86	0.83
		Townsville		
1987 (MSA)	0.67	0.57	0.10	0.48
1996 (LSA)	0.42	0.50	0.29	0.57
2001 (HSA)	0.46	0.76	0.66	0.61

4. Discussion

The high values of f_oE_s during daytime of local summers for all years under study over the three locations is a prevalent trend of sporadic E. Similar occurrences have been reported by several workers including Didebulidze

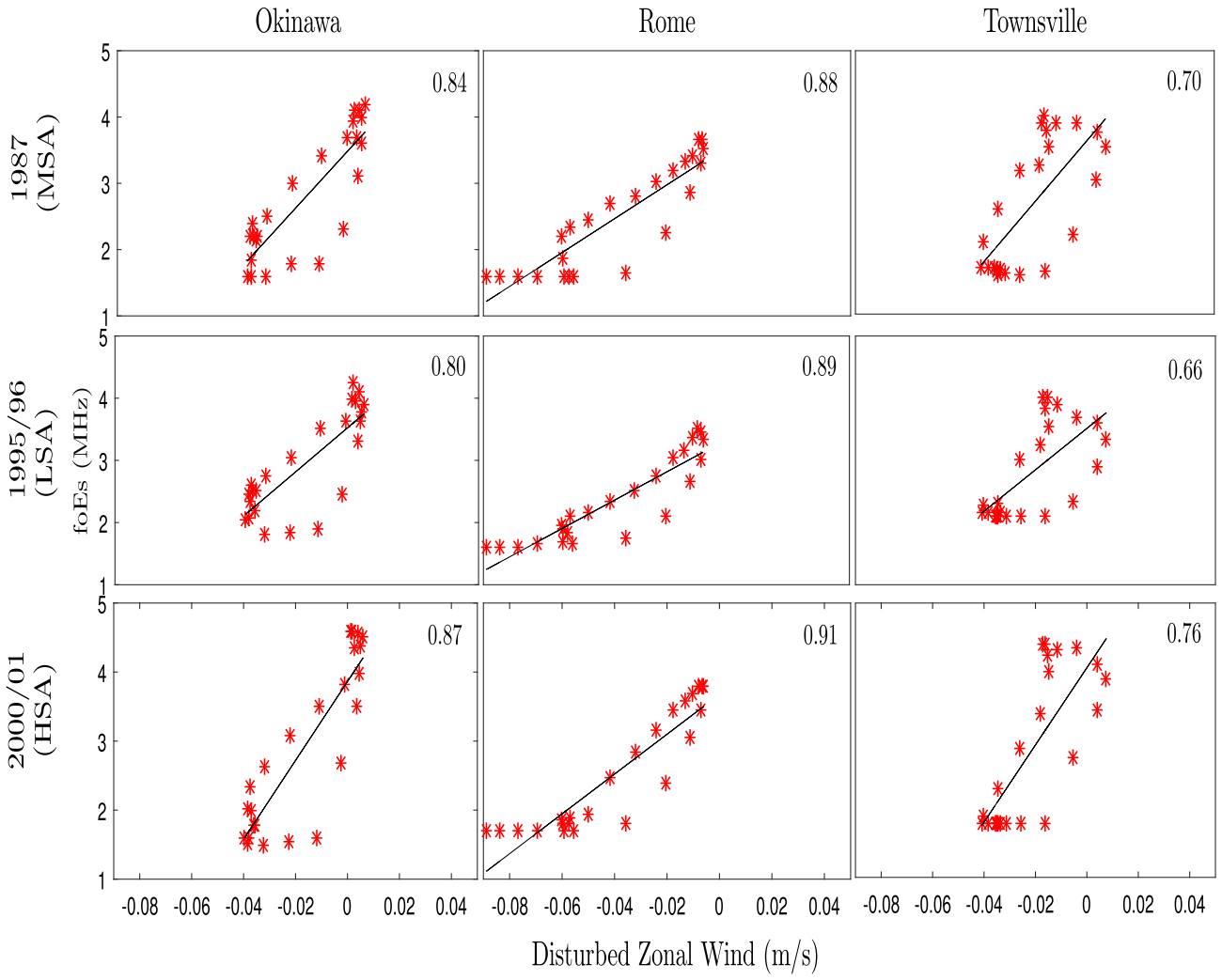

Fig. 2. Relation between f_oE_s and dzw at different observatories during different levels of solar activity. Each point corresponds to an hourly annual medians of both parameters. The number in each panel shows the correlation coefficient obtained. The coefficients of trend line between the variables are given in Table 4.

and Lomidze (2010), Davies (1990), Pietrella and Bianchi (2009). For Rome, the occurrence of this mid-latitude sporadic-E is most likely due to vertical shears in the horizontal neutral wind, which causes the combined action of ion-neutral collisional coupling and Lorentz forces compel the metallic ions to move vertically and converge into thin and dense plasma layers (Whitehead, 1989; Haldoupis et al., 2006). These shears are characterized (for the northern hemisphere) by a westward wind above and an eastward, or smaller westward, wind below as reported in the work by Haldoupis et al. (2006).

Table 4
Linear regression coefficients as defined by Eq. 2 for the data shown in Fig. 2.

	Rome	
	a	*b*
1987 (MSA)	25.54	3.48
1995 (LSA)	22.70	3.26
2000 (HSA)	28.82	3.67
	Okinawa	
1987 (MSA)	42.61	3.51
1996 (LSA)	35.44	3.53
2001 (HSA)	57.11	3.86
	Townsville	
1987 (MSA)	45.73	3.61
1996 (LSA)	33.29	3.51
2001 (HSA)	56.26	4.05

The annual correlation coefficient of f_oE_s with disturbed zonal wind obtained at mid-latitudinal region (Rome) is 0.91. From this high correlation coefficient, we infer that zonal winds may be related to the long hour existence (Maeda and Heki, 2015) (more than 5 h) of f_oE_s as found by Pietrella et al. (2014). Also, E_s-layers in mid-latitude regions are considered to be formed under vertical wind shear (Whitehead, 1989). Vertical shear of zonal winds drive upward and downward ion motions from layers below and above the E_s height, respectively (Larsen et al., 1998; Larsen, 2002; Haldoupis, 2012). The East–West

elongation of frontal structures may reflect the shape of the region where vertical shear of zonal winds exist.

Visibly higher values of f_oE_s occurrence at Okinawa is prevalent, which is due to the fact that *dzw* reaches its peak value in the sub-auroral regions at earlier local times during more active periods. The same feature has also been deduced from WINDII observations Emmert et al. (2004). It may be deduced that wind shear theory includes the influence of the horizontal magnetic field leading to a latitudinal dependence of E_s as reported by Jacobi et al. (2019).

As Mathews (1998) points out that the prevailing periodicities in mid-latitude sporadic E results from the confluence of the vertical tidal wind shears in the lower thermosphere, particularly in the altitude range between 100 km and 120 km. The observed diurnal periodicities seen in the occurrence, altitude descent and strength f_oE_s show the decisive role played by the atmospheric tides which provide the convergent wind shears needed for the layers to form and build up, while tidal phase progression downward causes their altitude descent.

The summer maximum is more pronounced in the northern hemisphere, which is due to the South Atlantic Anomaly and the weaker magnetic field there (Arras et al., 2010). Tanaka (1979) investigated local time dependence of the movements of E_s patches by radar backscatter observations. It was shown that northward and southward movements are dominant during 1000–1400 LT and 1500–2100 LT, respectively. This agrees with our results as shown in 1. E_s develops simultaneously over extended areas in space, rather than being a spatially restricted layer which is transported horizontally by neutral winds over a larger region (Rice et al., 2011).

Haldoupis (2011) supported the altitude dependency of zonal wind shear and reported that the ion-neutral collision frequency becomes progressively larger and particles become increasingly more demagnetized at lower sporadic E height (about 100–115 km) where ion convergence is mostly stable. This demagnetization negatively affects efficiency of meridional wind shear however zonal wind shear mechanism can still act to support ion convergence and thus sustain the presence of sporadic E-layer at lower heights as observed by Haldoupis and Shalimov (2021), recently. This explains the high correlation coefficients between f_oE_s and *dzw* of our study as we considered the effective height as 100 km. Furthermore, upon running a comparative analysis of correlation coefficients obtained through both quiet and disturbed zonal components of wind, a negative correlation (not shown in this manuscript) with quiet zonal wind validated our hypothesis that E_s-layer is formed by disturbed vertical wind-shear-driven metal ion transportation, where meteoric ionization contributes to ion formation in lower E-region.

Earlier, the geomagnetic field effect on layer formation was confirmed with more certainty by radio occultation such as the report by Igarashi et al. (2001). The radio occultation methodology can identify electron density perturbations in relation with strong sporadic E-layers and therefore measure the altitude and occurrence of sporadic E-layers. There are several radio occultation based studies of sporadic E that produced global maps of the occurrence of strong E_s situated below about 115 km. We refer here only to the report by Arras et al. (2010), which established a clear global relationship between strong low altitude E_s and geomagnetic field, whereas there exist several more relevant studies by other groups supporting the same finding. The radio occultation based studies confirmed the decisive role played by the Lorentz force in E_s generation by driving vertical ion convergence through the zonal wind shear mechanism. In addition, there is a growing list of studies where radio occultation sporadic E_s observations are combined with measured and modelled neutral winds in the lower E-region, to show that zonal wind shears there dominate the E_s-layer generation process, for example (Jacobi et al., 2019, and references therein).

The *dzw* at middle and low latitudes during daytime are mostly westward and the seasonal dependence is small (Fejer et al., 2000), therefore, in Table 3 we do not observe a notable seasonal dependency in both hemispheres. An earlier study by Xiong et al. (2015) implies that the disturbed wind propagates from high to low latitudes. During magnetically active periods the energy input from the solar wind into the upper atmosphere is most efficiently coupled into the high-latitude ionosphere-thermosphere system. Thus, the *dzw* reaches its peak value in the sub-auroral and mid-latitudinal region which is associated with enhanced plasma convection, therefore resulting in the highest annual correlation coefficient at Rome (0.91), higher at Okinawa (0.87) which is also a low-mid latitudinal region and the least at low latitudinal region, Townsville (0.76). The energy input from solar wind into the upper atmosphere subsequently causes the high latitude heating hence enhanced plasma drift synchronizing wind circulation (Xiong et al., 2015), therefore, the annual correlation coefficient should be the highest during magnetically active periods (decreasing from HSA to LSA).

5. Conclusion

We have reported the variation of f_oE_s and its relationship with disturbed zonal wind using HWM14 estimations. It is found that E_s-layer formation by *dzw* shows latitudinal dependency for the stations under study. This is because mid-latitudinal (Okinawa & Rome) E_s-layer appears to be more persistent at a height of 100 km where it remains stable for longer period of time hence resulting in the higher correlation coefficients. The critical frequency of E_s-layer does not show any significant dependence on solar activity. However, it shows annual trend with maximum values during local summers. From these results, it can be concluded that the HWM14 model can be used as a proxy to predict the climatology of the sporadic layers. This has been shown here using three ionosondes, taken as representative for different parts of the globe. In the

future, a more exhaustive study can be done along the same procedures that were demonstrated in-principle in this work.

Declaration of Competing Interest

The authors declare that they have no known competing financial interests or personal relationships that could have appeared to influence the work reported in this paper.

References

Arras, C., Jacobi, C., Wickert, J., Heise, S., Schmidt, T., 2010. Sporadic E signatures revealed from multi-satellite radio occultation measurements. Adv. Radio Sci. 8, 225–230. https://doi.org/10.5194/ars-8-225-2010.

Dalakishvili, G., Didebulidze, G.G., Todua, M., 2020. Formation of sporadic E (Es) layer by homogeneous and inhomogeneous horizontal winds. J. Atmos. Solar Terr. Phys. 209, 105403. https://doi.org/10.1016/j.jastp.2020.105403.

Davies, K., 1990. Ionospheric Radio. No. 31. The Institution of Engineering and Technology (IET), UK, doi: 10.1049/PBEW031E.

Davis, C.J., Johnson, C.G., 2005. Lightning-induced intensification of the ionospheric sporadic E layer. Nature 435 (7043), 799–801. https://doi.org/10.1038/nature03638.

Didebulidze, G.G., Dalakishvili, G., Todua, M., 2020. Formation of Multilayered Sporadic E under an Influence of Atmospheric Gravity Waves (AGWs). Atmosphere 11 (6), 653. https://doi.org/10.3390/atmos11060653.

Didebulidze, G.G., Lomidze, L.N., 2010. Double atmospheric gravity wave frequency oscillations of sporadic E formed in a horizontal shear flow. Phys. Lett. A 374 (7), 952–959. https://doi.org/10.1016/j.physleta.2009.12.026.

Drob, D.P., Emmert, J.T., Crowley, G., Picone, J.M., Shepherd, G.G., Skinner, W., Hays, P., Niciejewski, R.J., Larsen, M., She, C.Y., Meriwether, J.W., Hernandez, G., Jarvis, M.J., Sipler, D.P., Tepley, C. A., O'Brien, M.S., Bowman, J.R., Q. Wu, Y.M., Kawamura, S., Reid, I.M., Vincent, R.A., 2008. An empirical model of the Earth's horizontal wind fields: HWM07. J. Geophys. Res.: Space Phys. 113, A12304. https://doi.org/10.1029/2008JA013668.

Drob, D.P., Emmert, J.T., Meriwether, J.W., Makela, J.J., Doornbos, E., Conde, M., Hernandez, G., Noto, J., Zawdie, K.A., McDonald, S.E., Huba, J.D., Klenzing, J.H., 2015. An update to the Horizontal Wind Model (HWM): The quiet time thermosphere. Earth Space Sci. 2, 301–319. https://doi.org/10.1002/2014EA000089.

Emmert, J.T., Fejer, B.G., Shepherd, G.G., Solheim, B.H., 2004. Average nighttime F region disturbance neutral winds measured by UARS WINDII: Initial results. Geophys. Res. Lett. 31, L22807. https://doi.org/10.1029/2004GL021611.

Fejer, B.G., Emmert, J.T., Shepherd, G.G., Solheim, B.H., 2000. Average daytime F region disturbance neutral winds measured by UARS: Initial results. Geophys. Res. Lett. 27, 1859–1862. https://doi.org/10.1029/2000GL003787.

Haldoupis, C., 2011. A Tutorial Review on Sporadic E Layers, 381–394. https://doi.org/10.1007/978-94-007-0326-1_29.

Haldoupis, C., 2012. Midlatitude sporadic E. A typical paradigm of atmosphere-ionosphere coupling. Space Sci. Rev. 168, 441–461. https://doi.org/10.1007/s11214-011-9786-8.

Haldoupis, C., Meek, C., Christakis, N., Pancheva, D., Bourdillon, A., 2006. Ionogram height-time-intensity observations of descending sporadic E layers at mid-latitude. J. Atmos. Solar Terr. Phys. 68, 539–557. https://doi.org/10.1016/j.jastp.2005.03.020.

Haldoupis, C., Shalimov, S., 2021. On the altitude dependence and role of zonal and meridional wind shears in the generation of E region metal ion layers. J. Atmos. Solar Terr. Phys. 214, 105537. https://doi.org/10.1016/j.jastp.2021.105537.

Igarashi, K., Nakamura, M., Wilkinson, P., Wu, J., Pavelyev, A., Wickert, J., et al., 2001. Global sounding of sporadic E layers by the GPS/MET radio occultation experiment. J. Atmos. Solar Terr. Phys. 63, 1973–1980. https://doi.org/10.1029/2001JA900158.

Jacobi, C., Arras, C., Geißler, C., Lilienthal, F., 2019. Quarterdiurnal signature in sporadic E occurrence rates and comparison with neutral wind shear. Ann. Geophys. 37, 273–288. https://doi.org/10.5194/angeo-37-273-2019.

Larsen, M.F., 2002. Winds and shears in the mesosphere and lower thermosphere: Results from four decades of chemical release wind measurements. J. Geophys. Res.: Space Phys. 107 SIA 28-, 1–14. https://doi.org/10.1029/2001JA000218.

Larsen, M.F., Fukao, S., Yamamoto, M., Tsunoda, R., Igarashi, K., Ono, T., 1998. The SEEK Chemical Release Experiment: Observed neutral wind profile in a region of sporadic E. Geophys. Res. Lett. 25 (11), 1789–1792. https://doi.org/10.1029/98GL00986.

Maeda, J., Heki, K., 2015. Morphology and dynamics of daytime mid-latitude sporadic-E patches revealed by GPS total electron content observations in Japan. Earth, Planets Space 67 (1), 1–9. https://doi.org/10.1186/s40623-015-0257-4.

Mathews, J., 1998. Sporadic E: current views and recent progress. J. Atmos. Solar Terr. Phys. 60 (4), 413–435. https://doi.org/10.1016/S1364-6826(97)00043-6.

Pietrella, M., Bianchi, C., 2009. Occurrence of sporadic-E layer over the ionospheric station of Rome: analysis of data for thirty-two years. Adv. Space Res. 44 (1), 72–81. https://doi.org/10.1016/j.asr.2009.03.006.

Pietrella, M., Pezzopane, M., Bianchi, C., 2014. A comparative sporadic-E layer study between two mid-latitude ionospheric stations. Adv. Space Res. 54 (2), 150–160. https://doi.org/10.1016/j.asr.2014.03.019.

Piggott, W.R., Rawer, K., 1972. URSI Handbook of Ionogram Interpretation and Reduction. https://www.sws.bom.gov.au/IPSHosted/INAG/uag_23a/UAG_23A_indexed.pdf.

Plane, J.M.C., Self, D.E., Vondrak, T., Woodcock, K.R.I., 2003. Laboratory studies and modelling of mesospheric iron chemistry. Adv. Space Res. 32, 699–708. https://doi.org/10.1016/S0273-1177(03)00401-0.

Rice, D.D., Sojka, J.J., Eccles, J.V., Raitt, J.W., Brady, J.J., Hunsucker, R.D., 2011. First results of mapping sporadic E with a passive observing network. Space Weather 9. https://doi.org/10.1029/2011SW000678.

Schunk, R., Nagy, A., 2009. Ionospheres: Physics, Plasma Physics, and Chemistry. Cambridge University Press. https://doi.org/10.1017/CBO9780511635342.

Tanaka, T., 1979. Sky-wave backscatter observations of sporadic-E over Japan. J. Atmos. Terr. Phys. 41, 203–215. https://doi.org/10.1016/0021-9169(79)90013-8.

Whitehead, J.D., 1989. Recent work on mid-latitude and equatorial sporadic-E. J. Atmos. Terr. Phys. 51, 401–424. https://doi.org/10.1016/0021-9169(89)90122-0.

Xiong, C., Lühr, H., Fejer, B.G., 2015. Global features of the disturbance winds during storm time deduced from CHAMP observations. J. Geophys. Res.: Space Phys. 120, 5137–5150. https://doi.org/10.1002/2015JA021302.